Monitoring of the Heterogroup Twisting Dynamics in Phenol Type Molecules via Different Characteristic Free-Electron-Transfer Products

Ortwin Brede,* Ralf Hermann, Wolfgang Naumann, and Sergej Naumov†

Interdisciplinary Group for Time-Resolved Spectroscopy, University of Leipzig, Permoserstrasse 15, D-04303 Leipzig, Germany, and Institute of Surface Modification, D-04303 Leipzig, Germany

Received: August 29, 2001; In Final Form: December 4, 2001

Phenol radical cations as well as phenoxyl radicals were observed as direct products of free electron transfer from phenol type solute molecules to solvent parent radical cations generated by ionizing irradiation. It is shown that the finding of the two species in comparable amounts can be explained by a nuclear-structure dependent solute cation dissociation behavior: Quantum-chemical calculations indicate that for phenol as solute primarily its conformers with perpendicular C−OH axis orientation to the aromatic ring tend to prompt deprotonation after ionization. A quite similar behavior could be predicted also for the heteroanalogous thiophenols and selenophenols. Quite generally considerable changes in the electron distribution of the ground-state molecules with the twisting angle of the −OH, −SH and −SeH groups could be calculated, with the greatest differences between "parallel" and "perpendicular" conformations. On the assumption that the fast electron-transfer projects the equilibrium solute conformer distribution onto the solute cation conformer one it is demonstrated that the experimental findings are compatible with a simple solute-cation internal relaxation model. By applying the quantum-chemically calculated conformer interconversion barrier heights it can be understood that radical fraction among the direct products increases if phenols are substituted by thiophenols or those by selenophenols, as observed in experiment.

1. Introduction

Radiation-induced electron transfer in solutions offers a convenient way for producing radical cations ($S^{\cdot+}$) of a high variety of solute (donor or scavenger) molecules.[1−3] As well studied for *n*-alkanes,[4] cycloalkanes,[5] and alkyl chlorides, such as butyl chlorides,[6] dichloroethane,[7] and carbon tetrachloride,[8] in nonpolar solvents RX, the formed metastable parent ions react as a rule diffusion-controlled with solutes of lower ionization potential [reactions 1 and 2].

$$RX \text{ -vvv}\rightarrow RX^{\cdot+}, \quad e^-_{solv.}, \quad \text{radicals, etc.} \quad X = H, Cl \qquad (1)$$

$$RX^{\cdot+} + S \rightarrow S^{\cdot+} + RX \qquad (2)$$

It was recently found that using phenols (ArOH) or hetero analogous thiophenols and selenophenols as solutes, additionally to the expected radical cations ($ArOH]^{\cdot+}$) in a comparable amount also heteroatom centered radicals (phenoxyls, ArO·) are formed as direct products of the electron-transfer eq 2,[9−12] as expressed by the kinetic scheme

$$\mathbf{RX}^{\cdot+} + ArOH \rightarrow \mathbf{ArOH}]^{\cdot+}, \quad \mathbf{ArO}^{\cdot}, H^+, + RX \qquad (3)$$

where the directly observed species are in bold-face.

Sure experimental evidence that $ArOH]^{\cdot+}$ and ArO· in the sense of eq 3 indeed simultaneously arise was derived from the time profiles which demonstrated that for a reasonable phenol concentration of 5×10^{-3} mol dm^{-3} the reaction is complete in about 20 ns indicating an electron-transfer constant $k_3 = (1-2) \times 10^{10}$ dm^3 mol^{-1} s^{-1}. According to the hitherto existing radiation-chemical experience, no other reaction channel than an ionic one can in this time range compete with the transfer reaction. In particular, this is undoubtedly true for alkyl chlorides as solvent for which radiation-generated electronically excited states can be excluded. Moreover, intensive pulse radiolytic studies with differently structured phenols,[11,12] thiols,[10,12] and selenophenols as solutes revealed some unexpected and surprising results as to the product distribution of reaction 3 and its dependence on the solvent surrounding, pointing to a partial prompt deprotonation of the solute cations immediately after generation.

In this paper we start with a short summary of our already published experimental observations. It is then shown that the experimental finding of both phenol radical cations and phenoxyl radicals species as direct products of the electron transfer can be attributed to a structure-dependent solute-cation dissociation behavior. Results of quantum-chemical calculations are reported which indicate that conformers with a perpendicular C−OH axis orientation to the aromatic ring are clearly favored for a fast deprotonation. Quite similar dissociation behaviors can be predicted for the hetero analogous thiophenols and selenophenols. On the basis of these theoretical results it will be shown that different from a former hypothesis[12] the surprising experimental findings can be understood in the framework of a kinetic model which besides the solute−cation internal relaxation also takes the interconversion of their conformers into account. It is demonstrated that the quantum-chemically calculated conformer interconversion barrier heights allow at least qualitatively to explain why the radical part of the direct products increases if phenols are substituted by thiophenols or these by selenophenols, as observed in experiment.

† Institute of Surface Modification.

10.1021/jp013334z CCC: $22.00
Published on Web 01/22/2002

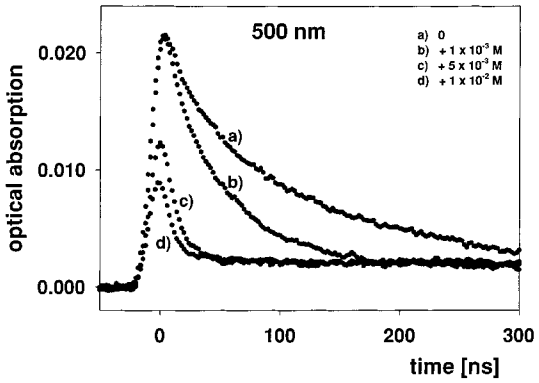

Figure 1. Time profiles from the pulse radiolysis of solutions of 4-methyl-2,6-di-*tert*-butyl-phenol in 1,2-dichloroethane purged with nitrogen. The figure reflects the effect of the increasing phenol concentration on the signal of the solvent radical cation.

2. Results of Pulse Radiolysis Experiments

Pulse radiolysis was performed with an ELIT type accelerator and an usual system for detection by optical absorption spectroscopy which is described in detail elsewhere.[13,14] The parameter of the system were as follows: pulse length 12 ns (fwhm), energy 1 MeV, dose per pulse between 50 and 100 Gy. Although in part separately published, the experimental facts are briefly concluded now.

After pulsing solutions of phenols in different saturated nonpolar solvents, the ion−molecule reaction 3 could be directly characterized by time-resolved optical absorption spectroscopy from the reactant as well as the product side. Already at phenol concentrations of 5×10^{-4} mol dm^{-3}, with decaying solvent ion RX$^{\cdot+}$ both products ArOH$]^{\cdot+}$ and ArO$^{\cdot}$ arise with a diffusion-controlled rate for all used donors. This procedure was carried out with different solvents such as cyclohexane, n-dodecane, *n*-butyl chloride and 1,2-dichloroethane, in each case with the same features.[11,12] Figure 1 demonstrates the observed behavior for the example of the pulse radiolysis of a solution of 4-methyl-2,6-di-tertbutyl-phenol in 1,2-dichloroethane. With increasing phenol concentrations the time profiles of the solvent radical cations shorten in sense of the pseudo-first-order reaction 3 resulting in a rate constant of about $k_3 = 9 \times 10^9$ dm^3 mol^{-1} s^{-1}. Such diffusion-controlled rate constants could generally be derived for all solvents and phenols studied.

From the product side, because of spectral superpositions the formation time profiles do not so clearly reflect the solvent radical cation decay. The product spectra are given in Figure 2 for a solution of 10^{-2} mol dm^{-3} 4-methyl-2,6-di-tertbutyl-phenol in 1,2-dichloroethane. By adding 0.1 mol dm^{-3} ethanol, the phenol radical cation part of the signal is completely quenched and only phenoxyl radicals survive. Figure 3a and b show the time profiles, taken in the two characteristic transient maxima at $\lambda = 400$ nm (ArO$^{\cdot}$) and $\lambda = 440$ nm (ArOH$]^{\cdot+}$), which despite the presence of a partial spectral superposition clearly reflect the different decay behavior of the phenoxyl radical and the phenol radical cation.

Whereas the phenoxyl radicals behave as quite stable species the promptly generated phenol radical cations further decay by deprotonation (reaction 4) in the time range of some hundred nanoseconds,[15] with a rate clearly depending on solute electronic structure (i.e. on the nature of the para substituents). Certainly, products of this reaction are delayed and therefore time-resolved formed phenoxyls.

$$\mathrm{ArOH}]^{\cdot+} \rightarrow \mathrm{ArO}^{\cdot} + \mathrm{H}^{+}_{\mathrm{solv.}} \qquad (4)$$

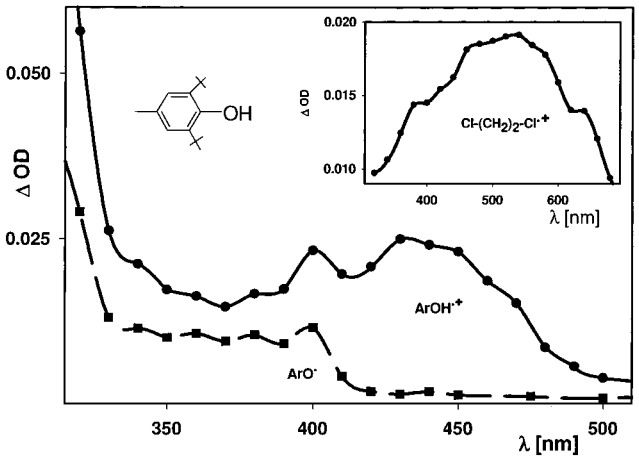

Figure 2. Transient optical absorption spectra of the phenol species, observed 50 ns after the electron pulse for a solution of 10^{-2} mol dm^{-3} 4-methyl-2,6-di-*tert*-butyl-phenol in 1,2-dichloroethane (●), attributed to ArOH$^{\cdot+}$ and ArO$^{\cdot}$. After adding 0.1 mol dm^{-3} of ethanol only the spectrum of ArO$^{\cdot}$ (■) remains. The inset shows the spectrum of the 1,2-dichlorethane radical cation taken in the nitrogen purged pure solvent.

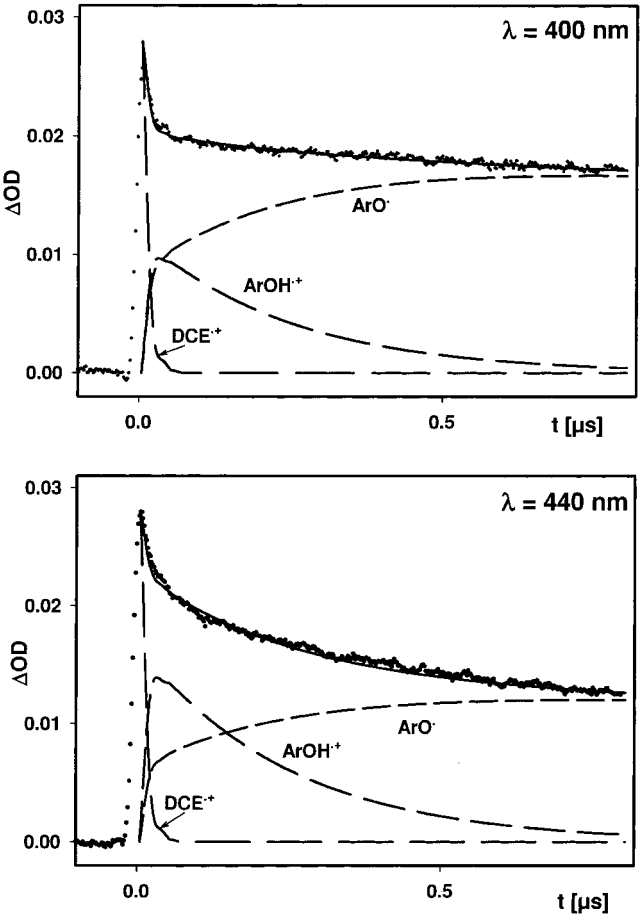

Figure 3. Time profiles of the phenol species taken in the pulse radiolysis of a solution of 10^{-2} mol dm^{-3} 4-methyl-2,6-di-*tert*-butyl-phenol in 1,2-dichloroethane purged with nitrogen: (a) at $\lambda = 400$ nm the ArO$^{\cdot}$ absorption dominates. (b) at $\lambda = 440$ nm the profile is taken in the ArOH$^{\cdot+}$ absorption maximum. The kinetic behavior of the transients contributing to the sum absorption time profiles is described by the fit curves obtained as described in detail in ref 11.

From the ratio between promptly (reaction 3) and delayed formed (reaction 4) ArO$^{\cdot}$, cf. Figure 3, the product distribution in the electron transfer (reaction 3) could be calculated.[12] For

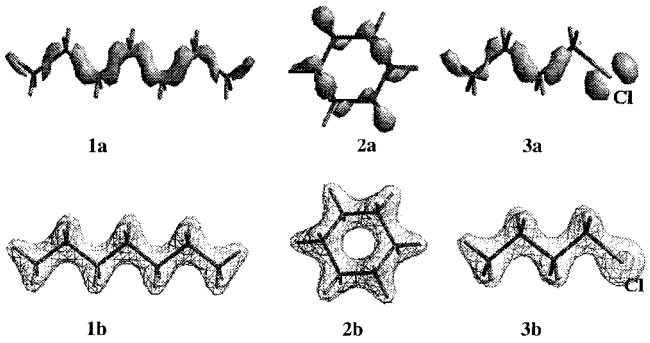

Figure 4. Quantum-chemical calculation (B3LYP/6-31G(d)) of parent solvent radical cations derived from *n*-heptane, cyclohexane, and *n*-butyl chloride: (a) total spin density surface (isospin = 0.01), (b) total charge density surface (isocharge = 0.1).

TABLE 1: Average Product Ratio (in Percent) of the Electron-Transfer Reaction 3 in the Solvents c−C_6H_{12}, *n*-$C_{12}H_{26}$, *n*-C_4H_9Cl, and 1,2-C_2H_4Cl

donor, ArOH or ArSH	$ArOH]^{\cdot+}$	$ArSH]^{\cdot+}$	ArO·	ArS·
phenol	49		51	
4-chlorophenol	50		50	
4-chlorophenol-OD	50		50	
4-methoxyphenol	50		50	
4-methyl-2,6-di-*tert*-butylphenol	51		49	
n-octadecyl-(3,5-di-*tert*-butyl-4-hydroxyphenyl)propionate	53		47	
thiophenol		34		66
4-methylthiophenol		34		66
4-methoxythiophenol		44		56
4-hydroxythiophenol	∼20		∼40	∼40
selenophenol, ArSeH	∼20 ($ArSeH]^{\cdot+}$)		∼80 (ArSe·)	

the different used phenols we found a ratio of 1:1, and this nearly independent of the electronic donor structure. A similar set of experiments with different aromatic thiols and with selenophenol reflected changed but also nearly constant product ratia for each heterophenol type (see Table 1).[12,16] If any, a little deviation from this general behavior could be observed for the long-tail substituted phenol. But this is not a very significant effect.

3. Analysis of the Observed Electron-Transfer Phenomenon

3.1. Properties of the Solvent Parent Ions. Compared with sensitized electron-transfer reactions,[17,18] in saturated nonpolar solutions the radiation-induced reactions between free solvent radical cations and solutes, called free electron transfer (FET), show some peculiarities. The parent radical cations in these solvents represent completely saturated σ-bonded molecules with the electron deficit (positive charge) regularly distributed over the whole molecule. In case of a high reactivity such species are often called positive holes. After their generation in the primarily nonrelaxed state, these holes exhibit an extremely high mobility as directly characterized by microwave conductivity experiments[19,20] or by UV−vis spectroscopical analysis[21,22] of the transfer reaction indicated in eq 5. This reaction was found to pass with rate constants up to two orders in magnitude higher than diffusion-controlled reactions of molecular ions. Among the possible explanations of that unusual behavior, something like resonance transfer or a residual excitation of the solvent ions (only for cycloalkanes and in a restricted sense for alkanes) comes into question. In the nanosecond time range the relaxed alkane radical cations (reaction 6) should behave as molecular ones but yet highly reactive species.

$$\oplus, RH + S \rightarrow S^{\cdot+} + RH, \quad \text{hole scavenging (S)} \qquad (5)$$

$$\oplus, RH \rightarrow RH^{\cdot+}, \quad \text{hole relaxation} \qquad (6)$$

It is known[1,2] that the characteristic features commonly found in *n*-alkanes and cycloalkane cation radicals are delocalization of the unpaired electron and positive charge all over the molecular frame (cf. Figure 4). Quantum-chemical calculations confirm a similar trend in the positive charge distribution also for cation radicals containing heavy atoms such as, e.g., chlorine in alkyl chlorides. Figure 4 demonstrates for the examples of *n*-heptane, cyclohexane and *n*-butyl chloride molecules that the unpaired electron is not really localized and the positive charge is spread throughout the whole molecule. For such a charge distribution an unhindered electron transfer (reaction 2) can be assumed proceeding in every encounter configuration of the reactants and being not restricted to any energetically preferred geometry. Therefore, as a special variant of an electron-transfer process, this free electron transfer (FET) shows a number of pecularities as listed below:[11,12]

(i) The FET occurs only in nonpolar solvents where the parent radical cations are metastable for kinetically reasonable times (between 10 and 200 nanoseconds).

(ii) Because of the mentioned charge distribution in the corresponding radical cations, the term "encounter complex" has to be taken more in sense of a supermolecule formed by the approaching reactants, and connected with a rapid electron transfer.

(iii) According to the electron-transfer theory,[25] in low polar solvents the majority of the excess (reorganization) energy of reaction 2 should especially be deposited in the vibrational modes of the reactants wheras the solvent reorganization is of minor importance.

(iv) As typical of most electron-transfer types, the change of the electronic state in the transfer step is rapid compared with the time necessary for nuclear rearrangements in the reactant molecules (Franck−Condon principle). Following some data in the literature,[26] it can be assumed that the real electron-transfer step is much faster than sensitized (photosensitized) processes.

Hence, for analyzing the free electron-transfer phenomenon under discussion, the process should be divided into three main steps:[12] (i) diffusive approach of the reactants, (ii) encounter formation and electron jump, and (iii) the internal relaxation of the products affecting the further fate of the product. The diffusion is considered to be by far the slowest process. After encounter formation, the real electron jump is assumed as a very fast step which because of the particular structure of the parent ions and of the high excess energy of the reaction should not be hindered by geometrical or electronic barriers. Compared with the rate of intramolecular electron exchange in aromatic systems (ring current),[27] for the electron-transfer step (ii) itself jump times of around 10^{-15} s can be assumed. This is important in connection with the interpretation of the phenol ionization (reaction 3) discussed later on in detail.

3.2. Radiation-Induced Electron Transfer from Phenol Type Molecules. Generally, the primary product of the electron transfer should be considered to be an at least vibrationally excited donor radical cation, certainly also in the case of the phenol type molecules. To interpret the unusual product distribution of reaction 3, the observed products suggest at least two suppositions as to the reaction channels, either concerning the relaxation of the product radical cation or even the preceding

TABLE 2: DFT B3LYP/6-31G(d) (Scale Factor $f = 0.96$) Calculated Frequencies of Polar XH group Rotation and Valence X−H Oscillations for ArXH (X = O, S, and Se), t = Times of One Motion.

ArOH			ArSH			ArSeH		
ν (cm^{-1})	t [10^{-15}s]	type	ν (cm^{-1})	t [10^{-15}s]	type	ν (cm^{-1})	t [10^{-15}s]	type
345	97	rotation	113	294	rotation	96	347	rotation
3601	9.3	O−H	2591	12.8	S−H	2260	14.8	Se−H

TABLE 3: B3LYP/6-311G(d,p) Calculated Thermochemistry Parameters for Stable and Transition States (ν_{min} Is the Minimum Frequency) of ArXH[a]

	n_{min}, cm^{-1}	structure	E_0, au	E_0 + ZPE, au	E_0 + ZPE + TE au	E_a, kcal/mol
Ar−OH 0°	+231	minimum	−307.55186	−307.44757	−307.44204	3.0
Ar−OH 90°	−357	tr.[b] state	−307. 54569	−307.44234	−307.43717	
Ar−SH 0°	+94	minimum	−630.52161	−630.42272	−630.41436	0.4
Ar−SH 90°	−50	tr. state	−630.52131	−630.42258	−630.41698	
Ar−SeH 0°[b]	−142	tr. state	−2633.85502	−2633.75792	−2633.75205	
Ar−SeH 90°[b]	+116	minimum	−2633.85499	−2633.75753	−2633.75096	0.7

[a] E_a is the activation energy of XH group rotation. [b] tr. = transition. [c] With 6-311+(d,p) basis set, because of Se atom.

electron jump step itself. The first and more common hypothesis is formulated by

$$RX^{\cdot+} + ArOH \rightarrow ArOH]^{\cdot+}* \rightarrow ArOH]^{\cdot+} + RX \quad (7a)$$

$$RX^{\cdot+} + ArOH \rightarrow ArOH]^{\cdot+}* \rightarrow ArO^{\cdot}, (H^+) + RX \quad (7b)$$

Here as an intermediate a uniform and planar structured transient radical cation in a vibrationally excited state is assumed which can decay by relaxation (reaction 7a) to the mentioned metastable cations (lifetime some hundred nanoseconds) or by deprotonation to phenoxyl radicals (reaction 7b). By means of this model, however, the constant ratio of the products also for very different electronically structured phenols (from the electron withdrawing p-Cl to the electron donating p-MeO) can hardly be understood (cf. Table 1). Furthermore, the solvent type (alkanes or alkyl chlorides) should affect the relaxation and, therefore, change the product situation. Hence this mechanism does not explain the experimental findings.

To understand how the observed constant product ratio for phenols with very different electronic structure (ranging from the electron withdrawing p-Cl to the electron donating p-MeO, cf. Table 1) can be explained, we theoretically investigated the electronic and nuclear structure of the phenols. Quantum-chemical analysis, as presented in the following section 3.3 reveals a critical electronic structure dependence on the twisting of the C−OH bond position relative to the aromatic ring, defining in this way different conformers (rotamers). Depending on the twisting barrier height and the excitation, a more or less hindered conformer interconversion will happen. For a sufficiently high barrier, as predicted for the phenols, the different conformers can effectively be taken for molecules which produce different cation electronic states immediately after ionization by electron transfer. In the following treatment it will be shown that for phenol a prompt deprotonation becomes only probable from ionized conformers with the C−OH axis sufficiently rotated out of the aromatic plane, as indicated by the following scheme

$$RX^{\cdot+} + ArOH_{plane} \rightarrow ArOH]^{\cdot+}* \rightarrow ArOH]^{\cdot+} \quad (8a)$$

$$\uparrow\downarrow$$

$$RX^{\cdot+} + ArOH_{rotat.} \rightarrow Ar{-}O^{\cdot+}{-}H]* \rightarrow ArO^{\cdot} + H^+ \quad (8b)$$

3.3. Calculations on the Molecular Dynamics of Phenol Type Molecules (ArXH) and of the Electron Distribution in the Derived Radical Cations (ArXH]$^{\cdot+}$). Quantum chemical calculations were done using the Gaussian 98, revision 9, program package.[28] The equilibrium geometries of the structures investigated were optimized completely without any restriction. Using the optimized structures the atomic charges as well as the atomic spin densities were calculated using the Mulliken population analysis. The Hartree−Fock (HF), Moller−Plesset (MP2), and density functional theory (DFT) Hybrid B3LYP[29−31] methods were used for investigation of the geometrical parameters and electronic structures of the ArXH (X = O, S, and Se) ground-state singlet and cation radical. All methods show the similar influence of the molecular geometry on electronic structure. The frequency calculations were used to locate transition state geometries, to determine the nature of stationary points found by geometry optimization, and to obtain thermochemistry parameters such as zero-point energy (ZPE), thermal correction to energy (TE), and activation energy E_a (height of rotation barrier). DFT is superior to other methods in reproducing vibrational frequencies for phenols.[32] Whereas the equilibrium geometries of the singlet ground state of ArOH and ArSH have a planar structure, the equilibrium geometries of the ArSeH (as calculated at B3LYP with standard 6-31G(d,p), 6-31G(3df,-3pd), 6-311G(d,p), and 6-311+G(d,p) basis sets) yield a stable conformer with the Se−H group perpendicular to the ring plane. The calculated data for the frequency analysis and the obtained thermochemical parameters are given in Tables 2 and 3.

The frequency job on the ArOH and ArSH stable planar structures produces no negative frequencies indicating that this conformation is a minimum one, whereas structures with the O−H and S−H group perpendicular to the ring plane (90°) produce only one negative (imaginary) frequency indicating that these conformations are first-order saddle points (transition states). In contrast, the frequency job on the ArSeH planar structures produces only one negative frequency indicating that this conformation represents the transition state, whereas the stable conformer with Se−H group rotated 90° to the ring plane has no negative frequency and, therefore, is the minimum.

As can be seen in Table 2, the valence X−H oscillations are at least 10 times faster than the rotation of the −XH group, but both of them are slow in comparison to the electron-transfer jump. Our calculated data of the phenol molecular oscillations are compatible with those given by Qin and Wheeler.[33]

Because of the small activation energies (barrier heights) E_a, for all three studied molecules a slowly internal rotation of XH group is possible. Within the Born−Oppenheimer approximation the molecular geometry is a stiff one relative to the electron relaxation process and a very fast electron-transfer event. To test the effect of the molecular geometry on the electronic

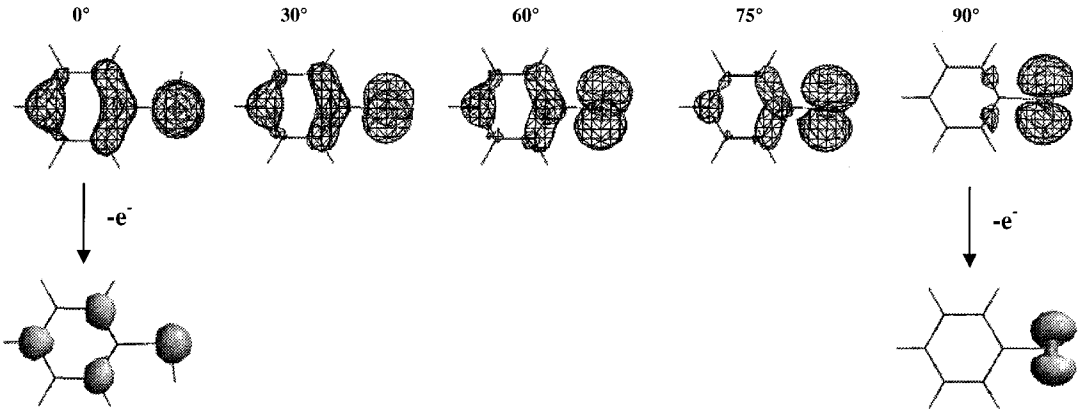

Figure 5. Transformation of HOMO of the ArSH singlet ground state (isocontour = 0.1) in dependence on SH group rotation and atomic spin density distribution of the ArSH cation radical (isospin = 0.01) as calculated with HF/6-31G(d) at B3LYP obtained geometry.

structure, we investigated the behavior of the highest double occupied MOs (HOMO) of the singlet ground state of ArXH, which are involved in electron-transfer process, in dependence on XH group rotation (with the torsion angle φ). For ArSH and ArSeH, the changes of electron distribution from HOMO show a similar trend (Figure 5). The S and Se atoms carry lone electron pairs and, therefore, are electron donors. In the planar structure lone pairs have similar impact as the π system of the aromatic ring. Due to the strong resonance with the π electron of the aromatic ring, the electron is shifted from the heteroatom to the aromatic moiety and the HOMO in the planar structure is delocalized over the whole molecule. By a rotation around the C−SH bond the coupling between ring and the lone pair electrons will be disturbed. Therefore the HOMO in the perpendicular structure has a *n*-symmetry and is almost entirely localized on the heteroatom of the polar group. Here it should be noticed that ArSH and ArSeH represent two marginal cases. While the stable structure of the thiophenol molecule is a planar one with a delocalized HOMO, the stable structure of selenophenol exhibits the Se−H group in a perpendicular position to the plane ring,[16] with a strongly localized HOMO.

Thus, due to the relatively slow rotation motion, after electron transfer from the HOMO of ArSH or ArSeH to the solvent radical cation (cf. refs 2 and 3), two different radical cations can be generated. In the first one, with planar structure, the charge is delocalized over the whole molecule. In the second, "perpendicular" radical cation the charge is strongly localized on the heteroatom. Thus, the perpendicular $ArXH]^{+}$ (X = S and Se) cation radical seems to be less stable than the planar one and is favored for a prompt deprotonation.

For phenols (ArOH) the situation is more complex and cannot be derived from the transformations of the HOMO only. Here we must consider the influence of steric interactions with bulky neighbor groups of the C−OH bond. It is known that the molecular orbital (MO) description can be used also for the interpretation of chemical phenomena. The electronic wave function (molecular orbital) ψ_i is defined for a particular molecular geometry. In the LCAO-MO model, MOs are formed as linear combinations of atomic orbitals (AO) φ_m ($\psi_i = SC_{mi}\varphi_m$). The effect of bond twisting on the MO energy (ϵ_i) can be estimated by first-order perturbation theory[34] with the formula

$$\delta_{\epsilon_i} = \Sigma_\mu \Sigma_\nu C_{\mu i} C_{\nu i} \beta_{\mu\nu}$$

where $\beta_{\mu\nu}$ denotes the bond twisting. ϵ_i becomes more positive if $C_{\mu i}$ and $C_{\nu i}$ have the same sign (bonding) and more negative if their signs differ (antibonding).

The steric strain in a π systems is relieved by rotation around formal single bonds. As can be seen for ArOH (Figure 6), the delocalized HOMO is antibonding between aromatic ring and oxygen atom and, as calculated by MP2/6-31G(d,p), negative values $C_{\mu i}C_{\nu i} = -0.047$ and -0.037 result (for 0° and 90°, respectively). It follows that the HOMO will be stabilized and drops down with an out-of-plane bond twisting. The HOMO-1 has no electron density between aromatic ring and oxygen atom and is not influenced by a bond twisting. At the same time HOMO-2 increases due to strong localization of the electron on the oxygen atom in the perpendicular structure and, therefore, the absolute value of $C_{\mu i}C_{\nu i}$ grows from -0.012 at 0° to -0.036 at 90°. Thus, if the OH group is perpendicular to aromatic ring, the three highest double occupied molecular orbitals are closer one to the others, i.e., the ionization potential differences become smaller.

As shown in Figure 6, in planar structure all three double occupied MO's have the same π symmetry with strongly delocalized electrons. In contrast, in the perpendicular structure only HOMO and HOMO-1 are delocalized. The HOMO-2 exhibits n-symmetry and is strongly localized on the oxygen atom. Starting from a MO scheme of a neutral closed shell phenol molecule (Figure 7), the ground configuration (a) and the excited configurations (b,c) of the corresponding radical cation (Koopmans configurations) can be achieved by a one step electron transfer.[35] Qualitatively comparing the planar and the perpendicular structures it can be seen that only the long-lasting delocalized radical cation can be built from the planar structure whereas in the perpendicular situation, because of the excess energy and the relatively small ionization potential difference, the electron transfer may happen also from HOMO-2, i.e., from the localized structure. Moreover, according to the frontier orbital theory[36] the interaction energy between electron donor and acceptor depends from the energy gap of the MOs as well as their overlapping. In the actual case because of the strong localization of the HOMO-2 electron, the overlap (and the charge-transfer integral) between the MOs of the reactants results in a favorable interaction energy, though the hypotheses of the electron transfer from HOMO-2 combined with the formation of a oxygen localized radical cation in the perpendicular structure seems to be justified.

Relating to these results, for a sufficiently short time scale were the rotation of the critical bond is "frozen" (femtosecond range) we can assume two limiting conformer structures strongly differing in the tendency for a prompt dissociation, in cor-

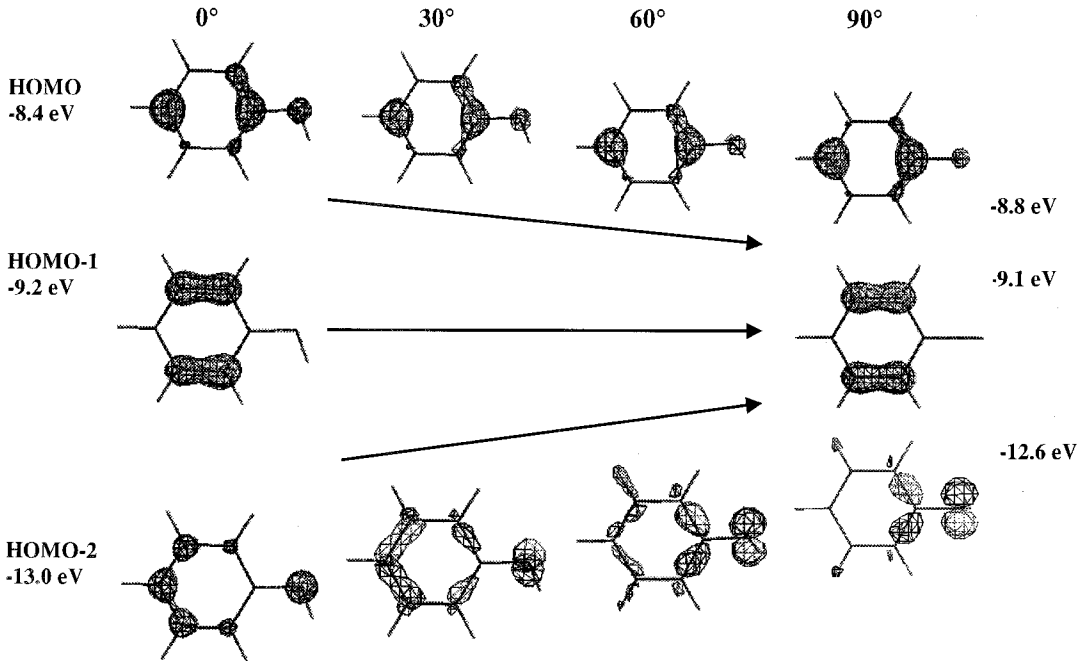

Figure 6. Transformation of HOMO, HOMO-1, and HOMO-2 of the ArOH singlet ground state (isocontour = 0.095) in dependence on the angle of the OH group rotation as calculated with MP2/6-31G(d,p).

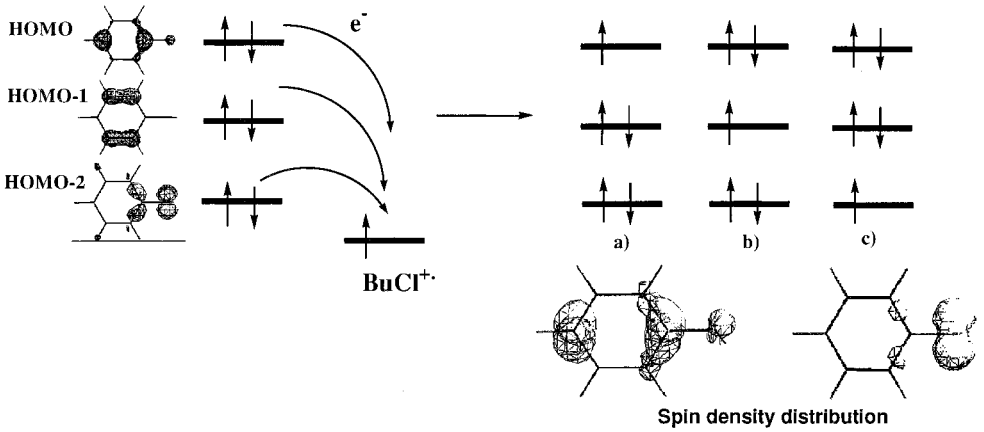

Figure 7. Molecular orbital scheme of the electronic configurations of the cation radicals formed by electron transfer from the perpendicular ArOH molecule to the solvent radical cation. Additionally, the atomic spin density distribution at planar and perpendicular structure of the ArOH cation radical are demonstrated ground and the excited state (isospin = 0.01) as calculated at UMP2/6-31G(d,p) level.

respondence with eq 8a,b. With this knowledge in mind, in the following chapter we will try a semiquantitative kinetic description.

3.4 Kinetic Treatment of the Deprotonation Kinetics. The experimentally observed radical formation over two well-separated time intervals ($10^{-14}-10^{-13}$ s vs 10^{-7} s) will be explained in the framework of a simple three-cation-state model on the basis of the condition that from the rapid electron-transfer reaction 3 due to the exothermicity of the reaction (corresponding to gas-phase solute−solvent ionization potential differences of $\Delta IP_g = 1.5-2.2$ eV[37]) rotationally and vibrationally excited solute cations arise.

(i) In rough consistence with the quantum-chemical structure calculations in section 3.2 we will assume for simplicity that immediately after the electron transfer two types of excited solute cation conformers (rotamers) must be distinguished, S_{1*} and S_{2*}, where only one type [say, S_{1*}] is favored for a prompt deprotonation, with an average dissociation constant k_{d*}.

Certainly, the quantum-chemically calculated parameters only allow a more or less qualitative estimation if the limiting rotamers, perpendicular or parallel, tend to deprotonation. Furthermore, the question is open how the dissociation type exactly depends on the intermediate values of the relevant twisting angle.

(ii) We further assume that competing with the fast deprotonation for S_{1*} type conformers, and more or less affected by an interconversion between S_{2*} and S_{1*} due to an −OH, −SH, or −SeH group twisting (internal rotation), the excited conformers will rapidly relax with a typical rate constant of $k_{rel} \sim 10^{11}$ s^{-1}.[38]

(iii) For the cation deprotonation in the thermally relaxed state [denoted in the following by S_0] we will assume an average dissociation constant k_d much smaller than k_{d*} and k_{rel}.

Here it should be mentioned that for deprotonation from an excited cation state in solutions the dissociation fragments (radical or proton) should have a much better chance to overcome the rate- and yield-reducing solvent cage effect[39,40] than that in the case of deprotonation from thermal equilibrium. This is obviously in line with the experimental observations of two strongly different rate constants.

The assumptions i−iii are reflected by the reaction scheme in Figure 8.

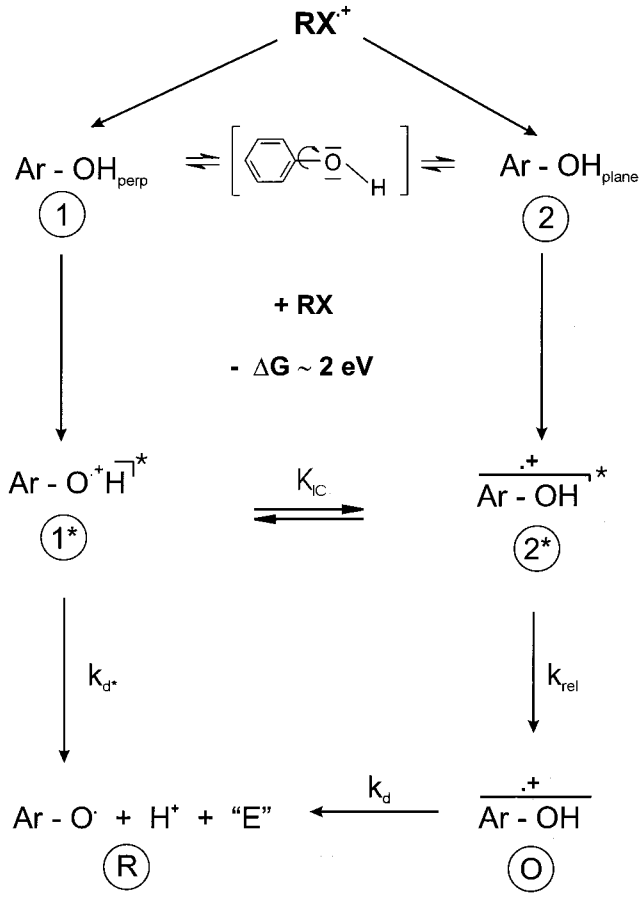

Figure 8. Reaction mechanism used for the kinetic description of the phenol radical cation relaxation. For symbolism, in the text the species are marked with the following understanding: S = ArOH, indexes of S_x agree with the circled numbers in the scheme.

If we denote the state-specific cation concentrations by C_{1*}, C_{2*}, and C_0 and the radical concentration by C_R, then according to our model assumptions i−iii for the kinetics after solute cation formation we can formulate the following rate equations

$$dC_{1*}/dt = -(k_{rel} + k_{d*})C_{1*}, \quad dC_{2*}/dt = -k_{rel}C_{2*} \quad (9)$$

$$dC_0/dt = k_{rel}(C_{1*} + C_{2*}) - k_dC_0, \quad (10)$$

$$dC_R/dt = k_{d*}C_{1*} + k_dC_0 \quad (11)$$

Denoting with p the fraction of excited radical cations which are formed from a fast deprotonation if k_{d*} is on the order of k_{rel} but both are much greater than k_d, eqs 9−11 compute the fraction of radicals formed during the solute radical cation deprotonation

$$p_R(t) = [\, k_{d*}\, p\, /(k_{d*} + k_{rel})]\{1 - \exp[-(k_{d*} + k_{rel})t]\,\} + [(k_{d*}(1-p) + k_{rel})(k_{d*} + k_{rel})\,]\{1 - \exp[-k_d\, t\,]\} \quad (12)$$

where the first term on the right-hand side essentially describes the radical formation during the "prompt" deprotonation. From formula 12 (which for the experimental interpretation has to be convoluted with the electron-transfer profile) follows, for a "frozen" rotamer interconversion during the solute cation relaxation, that the total fraction of promptly formed radicals is just proportional to the fraction $p \cong p_{eq}$ of the solute conformers in thermal equilibrium which are present as S_{1*} type cations immediately after ionization:

$$p_R^{\,fast} = k_{d*}p_{eq}/(k_{d*} + k_{rel}) \quad (13)$$

Assuming that p_{eq} can roughly be estimated from the quantum-chemically calculated −OH, −SH, and −SeH group twisting barriers E_a (cf. Table 3) by

$$p_{eq} \cong \exp(-E_a/kT\}/\,[1 + \exp(-E_a/kT\}] \quad (14)$$

we get $p_{eq} = 0.06$, 0.3, and 0.76 for the solute types ArOH, ArSH, and ArSeH, respectively. Note for this in accordance with the quantum-chemical calculations we assumed that the stable limiting conformations are planar ones for the phenols and thiophenols while the stable selenophenols demand a perpendicular SeH group orientation to the aromate. On the other hand the dissociative conformer state is a "perpendicular" one for all studied solute types.

These p_{eq}-values should be compared with the experimentally observed fractions of prompt deprotonation, $p_{exp} = 0.5$, 0.7, and 0.8 according to the dates in Table 1. The trend of a p_{exp} increase for going from the phenols over the thiophenols to the selenophenols is obviously in line with the estimated rising fraction of S_{1*} type conformers tending to fast deprotonation, while, however, the absolute p_{exp} and p_{eq} values considerably differ. The strong underestimation of the prompt deprotonation fraction of phenols by the theoretical parameter p_{eq} (estimated for frozen C−OH group rotation) indicates that either the radical yield increases by a possible conformer interconversion contribution during the solute cation excitation, or the experimental p-values are larger by an increased dissociation-fragment escape probability from the solvent cage by the cation excitation[39,40] immediately after generation, masking in this way the rotational barrier height dependence of the radical yield as expressed by the parameter p_{eq}.

4. Conclusion

Pulse radiolysis enabled the observation of products generated by fast electron transfer from phenol type molecules to parent solvent radical cations. Because of the extremely rapid electron jumps from the phenol to the parent ion, with nanosecond time resolution the process regularly finished within 50 ns under our conditions was characterized in something like a stationary manner, i.e., gives a product analysis only. The point of the nanosecond measurements, however, was the exclusive reduction of the reaction mechanism to the radiation-induced *electron transfer*.

It was demonstrated that the rapid electron transfer from phenolic solutes to the parent solvent ions yield two different direct products: phenol radical cations and phenoxyl radicals. Their generation is tightly connected with the existence of *two* different types of short-living solute cation intermediates which either relax to a relatively stable state or promptly deprotonate to the mentioned radicals. It could be excluded that only stable intermediates are reactive since then solely one product type has to be expected, (i) for thiophenols the long-lasting radical cation and (ii) for selenophenol the heteroatom centered radical, in contrast to the experiment.

From quantum-chemical calculations it could be followed that the observed rapid deprotonation monitors the presence of different solute conformers in effect, varying in case of phenol in the C−OH axis position to the aromatic ring. Regarding the calculated strongly different deprotonation behavior (especially of the "plane" and "perpendicular" cation conformers) it was shown that the experimentally observed time profiles can be understood with a solute−cation internal relaxation model.

Deriving the solute−conformer equilibrium distribution from the quantum-chemically calculated bond twisting barriers E_a it was demonstrated that the radical part of the direct products should increase if phenols are substituted by thiophenols or those by selenophenols, as exactly observed in experiment.

Nowadays such prompt and delayed dissociations of energy-rich organic molecules are in upcoming discussion. So the expected kinetic stability of larger molecules seems to be not necessarily the rule, and fast processes are possible as treated theoretically by Remacle and Levine.[41] In our case such a very short time scale electron-transfer induced event gives a deeper, experiment-based understanding of the molecular dynamics in liquid state.

Summarizing, we believe that our surprising observations are especially based on two kinetic aspects, on the fast formation of internally excited solute cations by a rapid (free) electron transfer and on their conformer-dependent dissociation behavior where the latter was monitored by the experiment.

References and Notes

(1) Brede, O.; Mehnert, R.; Naumann, W. *Chem. Phys.* **1987**, *115*, 279.

(2) Mehnert, R. in *Radical Ionic Systems−Properties in Condensed Phases*; Lund, A., Shiotani, M. Eds.; Kluwer Academic Publishers: Dordrecht, 1991; p 231.

(3) Guldi, D. M., Asmus, K.-D., *J. Am. Chem. Soc.* 1997, *119*, 9**,** 5744.

(4) Mehnert, R.; Brede, O.; Naumann, W. *Ber. Bunsen-Ges. Phys. Chem.* **1984**, *88*, 71.

(5) Mehnert, R.; Brede, O.; Naumann, W. *Radiat. Phys. Chem.***1985**, *26*, 499.

(6) Mehnert, R.; Brede, O.; Naumann, W. *Ber. Bunsen-Ges. Phys. Chem.* **1982**, *86*, 525.

(7) Spectra see Figure 2, for details: Brede, O. et al. To be published

(8) Mehnert, R.; Brede, O.; Bös, J.; Naumann, W. *Ber. Bunsen-Ges. Phys. Chem.* **83**, *1979*, 992. Brede, O.; Bös, J.; Mehnert, R. *Ber. Bunsen-Ges. Phys. Chem.* **1980**, *84*, 63.

(9) Brede, O.; Orthner, H.; Zubarev, V.; Hermann, R. *J. Phys. Chem.* **1996**, *100*, 7097.

(10) Hermann, R.; Dey, G. R.; Naumov, S.; Brede, O. *Phys. Chem. Chem. Phys.* **2000**, *2*, 1213.

(11) Mahalaxmi, G. R.; Hermann, R.; Naumov, S.; Brede, O. *Phys. Chem. Chem. Phys.* **2000**, *2*, 4947.

(12) Brede, O.; Ganapathi, M. R.; Naumov, S.; Naumann, W.; Hermann, R. *J. Phys. Chem. A* **2001**, *105*, 3757.

(13) Brede, O.; David, F.; Steenken, S. *J. Chem. Soc., Perkin Trans.2* **1995**, *2*, 23.

(14) Lomoth, R.; Naumov, S.; Brede, O. *J. Phys. Chem. A* 1999, *103*, 2641.

(15) Ganapathi, M. R.; Naumov, S.; Hermann, R.; Brede, O. *Chem. Phys. Lett.* **2001**, *337*, 335.

(16) Brede, O.; Hermann, R.; Naumov, S.; Mahal, H. S. *Chem. Phys. Lett.* **2001**, *350*, 165.

(17) Marcus, R. A. *Annu. Rev. Phys. Chem.* **1964**, *15*, 155 and subsequent papers.

(18) Rehm, D.; Weller, A. *Ber. Bunsen-Ges. Phys. Chem.* **1969**, *73*, 5834.

(19) (a) Zador, E.; Warman J. M.; Hummel, A. *Chem. Phys. Lett.* **1973**, *23*, 363. (b) de Haas, M.; Warman, J. M.; Infelta, P. P.; Hummel, A. *Chem. Phys. Lett.* **1975**, *31*, 382. (c) Warman, J. M.; Infelta, P. P.; de Haas, M. P.; Hummel, A. *Chem. Phys. Lett.* **1976**, *43*, 321. (d) de Haas, M. P.; Hummel, A.; Infelta, P. P.; Warman, J. M. *Can. J. Chem.* **1977**, *55*, 2249.

(20) Beck, G.; Thomas, J. K. *J. Phys. Chem.* **1972**, *76*, 3856.

(21) a) Brede, O.; Helmstreit W.; Mehnert R. *Chem. Phys. Lett.* **1974**, *28*, 43. (b) Brede, O.; Bös, J.; Naumann, W.; Mehnert R. *Radiochem. Radioanal. Lett.* **1978**, *35*, 85.

(22) For a review, see: Trifunac, A. D.; Sauer, M. C.; Shkrob, I. A.; Werst, D. W. *Acta Chem. Scand.* **1997**, *51*, 158.

(23) Toriyama, K. in *Radical Ionic Systems−Properties in Condensed Phases*, Lund, A., Shiotani, M., Eds.; Kluwer Academic Publishers: Dordrecht, 1991; p 99.

(24) Wang, P.; Shiotani, M.; Lunell, S. *Chem. Phys. Lett.* **1998**, *292*, 110.

(25) Bixon, M.; Jortner, J. *Adv. Chem. Phys.* **1999**, *106*, 35.

(26) Warman, J. M. in *The Study of Fast Processes and Transient Species by Electron Pulse Radiolysis*; Reidel Publishers: Dordrecht, 1982; p 433.

(27) Stiller, W. *Nichtthermisch aktivierte Chemie*; Birkhäuser Verlag: Basel, 1987; p 55.

(28) Frisch, M. J.; Trucks, G. W.; Schlegel, H. B.; Scuseria, G. E.; Robb, M. M. A.; Cheeseman, J. R.; Zakrzewski, V. G.; Montgomery Jr., J. A.; Stratmann, R. E.; Burant, J. C.; Dapprich, S.; Millam, J. M.; Daniels, A. D.; Kudin, K. N.; Strain, M. C.; Farkas, O.; Tomasi, J.; Barone, V.; Cossi, M.; Cammi, R.; Mennucci, B.; Pomelli, C.; Adamo, C.; Clifford, S.; Ochterski, J.; Petersson, G. A.; Ayala, P. Y.; Cui, Q.; Morokuma, K.; Malick, D. K.; Rabuck, A. D.; Raghavachari, K.; Foresman, J. B.; Cioslowski, J.; Ortiz, J. V.; Baboul, A. G.; Stefanov, B. B.; Liu, G.; Liashenko, A.; Piskorz, P.; Komaromi, I.; Gomperts, R.; Martin, R. L.; Fox, J.; Keith, T.; Al-Laham, M. A.; Peng, C. Y.; Nanayakkara, A.; Gonzalez, C.; Challacombe, M.; Gill, P. M. W.; Johnson, B.; Chen, W.; Wong, M. W.; Andres, J. L.; Gonzalez, C.; Head Gordon, M.; Replogle E. S.; Pople J. A. *Gaussian 98*, revision A9; Gaussian Inc., Pittsburgh, PA, **1998**.

(29) Becke, A. D. *J. Chem. Phys.* **1993**, *98*, 5648.

(30) Becke, A. D. *J. Chem. Phys.* **1996**, *104*, 1040.

(31) Lee, Ch.; Yang, W.; Parr, R. G. *Phys. Rev. B* **1987**, *37*, 785.

(32) Zierkiewicz, W.; Michalska, D.; Zeegers-Huykens, T. *J. Chem. Phys.* **2000**, *104*, 11685.

(33) Quin, Y.; Wheeler, R. A. *J. Phys. Chem.* **1996**, *100*, 10554.

(34) Klessinger, M.; Michl, J. *Lichtabsorption und Photochemie Organischer Moleküle***;** VCH: Weinheim, 1989; p 127.

(35) Bally, T. In *Radical Ionic Systems−Properties in Condensed Phases*, Lund, A., Shiotani, M., Eds.; Kluwer Academic Publishers: Dordrecht, 1991; p 4.

(36) (a) Klopman, G. *J. Am. Chem. Soc.* **1968**, *90*, 223. (b) Salem, L. *J. Am. Chem. Soc.* **1968**, *90*, 543.

(37) Lide, D. R., Ed. *Handbook of Chemistry and Physics*, 73rd Ed.; CRC Press: 1992; pp 10−220.

(38) Fujiwara, M.; Toyomi, K. *J. Chem. Phys.* **1997**, *107*, 9354.

(39) Beddard, G. *Rep. Prog. Phys.* **1993**, *56*, 63.

(40) Cattaneo, P.; Granucci, G.; Persico, M. *J. Phys. Chem. A* **1999**, *103*, 3364.

(41) Remacle, F.; Levine, R. D. *J. Phys. Chem. A* **1998**, *102*, 10195.